Journal of Sound and Vibration (1999) **222**(5), 753–779
Article No. jsvi1998.2085, available online at http://www.idealibrary.com on IDEAL®

ON THE GENERATION OF DISCRETE FREQUENCY TONES BY THE FLOW AROUND AN AEROFOIL

A. McALPINE*
School of Mathematics, University of Bristol, Bristol BS8 1TR, England
AND
E. C. NASH AND M. V. LOWSON
Department of Aerospace Engineering, University of Bristol, Bristol BS8 1TR, England

(*Received* 6 *April* 1998, *and in final form* 11 *November* 1998)

Tonal noise, the self-induced discrete frequency noise generated by aerofoils, is investigated. It is heard from an aerofoil placed in streams at low Mach number flows when inclined at a small angle to the stream. It is a piercing whistle, commonly up to 30 dB above the background noise level. Previous authors have attributed tonal noise to a feedback loop consisting of a coupling between laminar boundary-layer instability waves and sound waves propagating in the free stream. Boundary-layer measurements have shown the presence of tonal noise is closely related to the existence of a region of separated flow close to the trailing edge of the aerofoil. An analysis of the linear stability of the boundary-layer flow over the aerofoil is presented. The amplification of the instability waves is shown to be controlled almost entirely by the region of separated flow close to the trailing edge. In light of these new experimental and theoretical results the suitability of the aero-acoustic feedback model is discussed.

1. INTRODUCTION

This paper describes an experimental and theoretical investigation into the generation of noise of discrete frequency by aerofoils. The noise radiated from aerofoils is at certain flow conditions dominated by a piercing whistle which is at a discrete frequency, typically between 20 and 30 dB above the background broadband level. This phenomenon is thus often called ''tonal noise''.

Tonal noise is commonly heard from gliders, small aircraft, rotors and fans. Recently tonal noise has been reported to be a prevalent problem with wind-turbines. The problem of tonal noise from rotors and fans is more

*Present address: Institute of Sound and Vibration Research, University of Southampton, Southampton SO17 1BJ, England.

0022–460X/99/200753 + 27 $30.00/0

complicated than for a fixed aerofoil because each blade in a rotor or fan passes through the wake of its neighbouring blade during rotation. Therefore, in this paper tones are investigated from a single, fixed, isolated aerofoil to simplify the problem.

The first paper dedicated to the tonal noise generated by isolated aerofoils is believed to be that of Paterson *et al.* [1] in 1973. A hot-wire placed in the aerofoil wake, downstream of the trailing edge of the aerofoil, revealed large wake fluctuations at the same frequency as the acoustic tone. They believed the tones were caused by vortex shedding at the trailing edge, and that the tones were louder than other sources of (broadband) sound such as the turbulent boundary layer. The presence of the tone was associated with a laminar boundary layer up to the trailing edge on the pressure surface of the aerofoil. For small variations in the free-stream velocity U_∞, the frequency of the tones were approximately proportional to $U_\infty^{0{\cdot}8}$. At intermittently spaced free-stream velocities the frequency of the tone was observed to "jump" to other curves proportional to $U_\infty^{0{\cdot}8}$. The frequency of the tones against the free-stream velocity had a "ladder-like" structure with "rungs" of curves proportional to $U_\infty^{0{\cdot}8}$. Paterson *et al.* suggested that the tonal frequency f was dependent on the free-stream velocity U_∞ and the boundary-layer thickness δ at the trailing edge of the aerofoil. They assumed that the Strouhal number $St = 2f\delta/U_\infty$ was constant, and then predicted the tonal frequency by measuring U_∞ and δ. (Previous experimental work had shown that St was approximately constant for a *bluff* body.) This resulted in the scaling law $f \propto U_\infty^{3/2}$ which qualitatively described the average behaviour of the dependence of the tonal noise on the free-stream velocity.

In 1974, Tam [2] suggested that because an aerofoil was streamlined, this was a poor approximation to a bluff body with which vortex-shedding noise was commonly associated. He proposed that tonal noise was generated by a self-excited feedback loop located between the trailing edge of the aerofoil and a point downstream in the wake. Boundary-layer instabilities propagating into the wake would grow, causing the wake to vibrate laterally. These vibrations would emit an acoustic wave at some point close to the trailing edge which coupled with the instabilities propagating into the wake over the trailing edge—thus completing the loop. Using hydrodynamic stability theory, Tam calculated the total phase change around the loop. He proposed that for reinforcement to occur the phase change should be an integral multiple of 2π. The "ladder-like" structure observed by Paterson *et al.* could then be explained by changes in the total phase around the loop.

The aero-acoustic feedback loop proposed by Tam was modified by Wright in 1976 [3], Longhouse in 1977 [4], Fink in 1978 [5], and Arbey and Bataille in 1983 [6]. It was believed that aerodynamic disturbances (or boundary-layer waves) induced a fluctuating pressure distribution on the aerofoil surface which, on interacting with the sharp, trailing edge of the aerofoil, generated sound. Sound waves propagating upstream reinforced the original disturbance, thus completing the feedback loop. The loop was maintained if the sound had appropriate phase and magnitude to couple with the boundary-layer waves at the source point,

taken to be the location on the aerofoil where the boundary-layer waves became unstable.

Tonal noise also occurs in underwater applications, such as hydrofoils and propellers. Blake in 1986 [7] (see Chapter 11), and Blake and Gershfeld in 1989 [8], comprehensively reviewed the generation of aerodynamic sound by trailing edge flows. The occurrence of tonal and broadband noise due to vortex shedding and aero-acoustic scattering of boundary-layer turbulence was detailed with respect to the flow conditions and edge geometry. The wake of a blunt edged aerofoil forms a quasi-periodic vortex street, and the quality (i.e., sharpness) of the tonal noise depends upon the orderliness of the vortices close to the trailing edge. Typically, the amplitude of the tones from a blunt edged aerofoil are greater than with a sharp trailing edge. Classically (e.g., Paterson *et al.* [1]) the characteristics of these tones are presumed to be controlled by the wake. The frequency is predicted by using a Strouhal number mechanism (commonly associated with bluff bodies) based on the wake thickness of the vortex-street close to the trailing edge of the aerofoil.

In most of these papers it is assumed that the existence of tonal noise is dependent on a laminar boundary layer extending up to the trailing edge on the pressure surface of the aerofoil. Longhouse mentioned the possibility of flow separation on the aerofoil although this was not pursued any further. However, the flow separation on a NACA 0012 aerofoil had been reported in 1971 by Hersh and Hayden [9] when investigating sound radiation from lifting surfaces (although not specifically tonal noise).

Preliminary results from this current investigation in Lowson *et al.* in 1994 [10], and Nash and Lowson in 1995 [11] reported the occurrence of tonal noise was largely dependent on the existence of a laminar separation bubble (near the trailing edge) on the pressure surface of the aerofoil. There were large fluctuations around the separation bubble, fluctuations at the frequency of the tonal noise. They concluded that the fluctuations were amplified Tollmien–Schlichting (T–S) waves and the tonal frequencies were controlled by the region of separated flow.

Dovgal *et al.* in 1994 [12] reviewed laminar boundary-layer separation and its associated instability. They defined a separation bubble as the region of recirculating flow between the flow separation and re-attachment points on the surface of a rigid body. Experimental observations showed that separation bubbles were usually very small, often less than one boundary-layer thickness high, and that separated flows became unstable at relatively low Reynolds numbers. A separation bubble induces boundary-layer transition at or close to the point of re-attachment, where the transition originates from the strong growth of initially small-amplitude disturbances in the neighbourhood of the separation bubble. Dovgal *et al.* commented that the disturbances surprisingly appeared linear until their amplitude was about 1% of U_∞.

In this paper we concentrate on the stability of the boundary layer on the pressure surface of the aerofoil to enhance understanding of the relationship between T–S waves and tonal noise. The experimental results presented in the following section are included to compare with the theoretical results in sections

3 and 4. The comparisons are discussed in section 5, and we comment on the implications regarding the aero-acoustic feedback model.

The brief selection of experimental results presented in this paper were obtained by using a closed-loop, low-turbulence wind-tunnel in the Aerospace Engineering Laboratory at the University of Bristol. A complete summary of the experimental results, together with a detailed description of the wind-tunnel test facility and experimental techniques has been published by Nash *et al.* [13]. Also, see the paper by Nash and Lowson [11] for a description of the steps taken to eliminate the numerous spurious frequencies (e.g., Parker modes) associated with testing in a closed wind-tunnel.

2. EXPERIMENTAL INVESTIGATION

Experimental results were obtained by using a NACA 0012 and FX79 W151 aerofoil. The aerofoil cross-sectional profiles are shown in Figure 1. Note the NACA 0012 and FX79 W151 aerofoils had chord lengths of 300 and 230 mm, respectively.

The acoustic measurements were taken with a microphone mounted above, and downstream of, the trailing edge of the aerofoil. The wind-tunnel was driven for flow velocities between 5 and 70 ms^{-1}. The discrete tones detected were typically about 90 dB, i.e., up to 30 dB higher than the background broadband level.

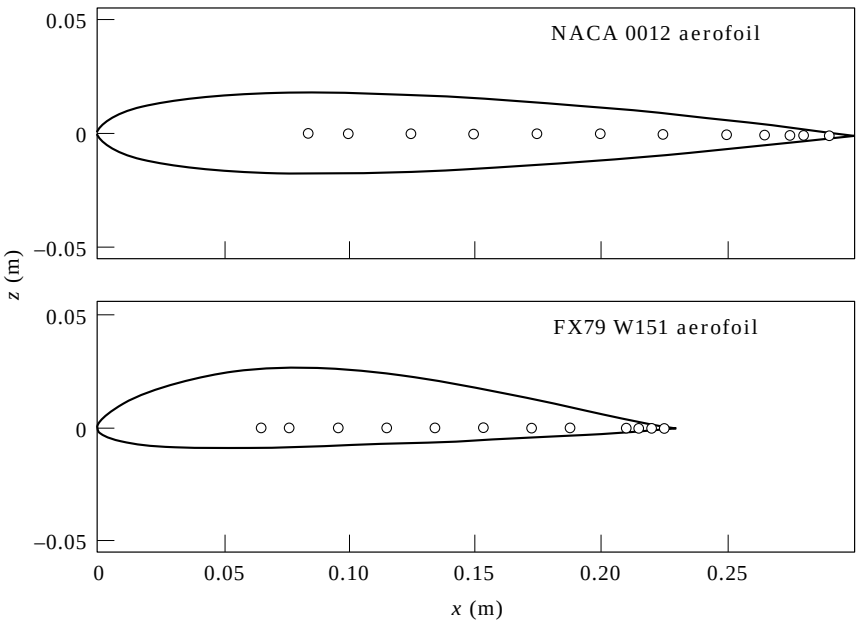

Figure 1. NACA 0012 and FX79 W151 aerofoils. The chordwise location of stations 1 to 12 where experimental results were obtained in cases 1 and 4 are denoted by ○. (Note that it was necessary to slightly alter the location of some of the stations in the other cases to positions where satisfactory experimental measurements were acheived.)

TABLE 1
Details of cases of tonal noise investigated

Case	Aerofoil	Angle (degrees)	U_∞ (ms^{-1})	Tone (Hz)
1	NACA 0012	−4	30	1048
2	NACA 0012	−4	38	1280
3	NACA 0012	−4	44	1420
4	FX79 W151	−3	30	1192
5	NACA 0012	−3	8	No tone
6	NACA 0012	0	17	No tone

Until recently the most common method of measuring boundary-layer flows was with a hot-wire anemometer. In this study a hot-wire was found to have two significant limitations. Firstly, a hot-wire is unable to detect the direction of the flow, and secondly, the hot-wire is a flow-intrusive measuring device. Nash (cf. reference [14], Chapter 6) found that the tonal noise mechanism was too sensitive to be studied by using a hot-wire because the hot-wire adversely affected the separation bubble. Hence, all the experimental results were obtained by using a laser doppler anemometer (LDA), which is a non flow-intrusive measuring device. In addition to measuring the boundary-layer profiles (see reference [13] for examples), spectral measurements were also taken by using the LDA.

In sections 3 and 4 the linear stability of the flow around the aerofoil is investigated for the cases outlined in Table 1. Note that the angle of the aerofoil to the oncoming stream is negative to facilitate access (the majority of the measurements were taken in the pressure surface boundary layer which was then on the top surface).

Tonal noise is detected over a range of free-stream flow velocities where the aerofoil is inclined at a small angle to the oncoming stream. For the NACA 0012 aerofoil inclined at $-4°$, tonal noise is detected for $20\ \text{ms}^{-1} < U_\infty < 60\ \text{ms}^{-1}$. However, at $0°$ no tonal noise is detected from the NACA 0012 aerofoil for all free-stream velocities. The sensitivity of the tonal noise mechanism to changes in the free-stream velocity and the angle of inclination is discussed in section 4, by using the results from cases 5 and 6.

Figure 2 shows the acoustic frequency spectra for the tonal cases 1–4. In each case the discrete tones are clearly visible above the background broadband level. (The loud, low frequency, broadband noise visible in each spectrum is due to extraneous tunnel noise.) The experimental results for cases 1–4 all exhibit the same features. There is a region of reversed flow close to the trailing edge of the aerofoil in each case. Typically the flow is attached and laminar until approximately 20 mm upstream of the trailing edge.

Figures 3–5 show frequency spectra taken in the centre of the boundary layer for cases 4, 5 and 6, respectively. For these cases, two frequency spectra are shown, one taken close to the trailing edge of the aerofoil and one further upstream. In Figure 3 there is a fundamental mode at 1192 Hz, the frequency of the tone, up to 30 dB above the background broadband level. The amplitude of

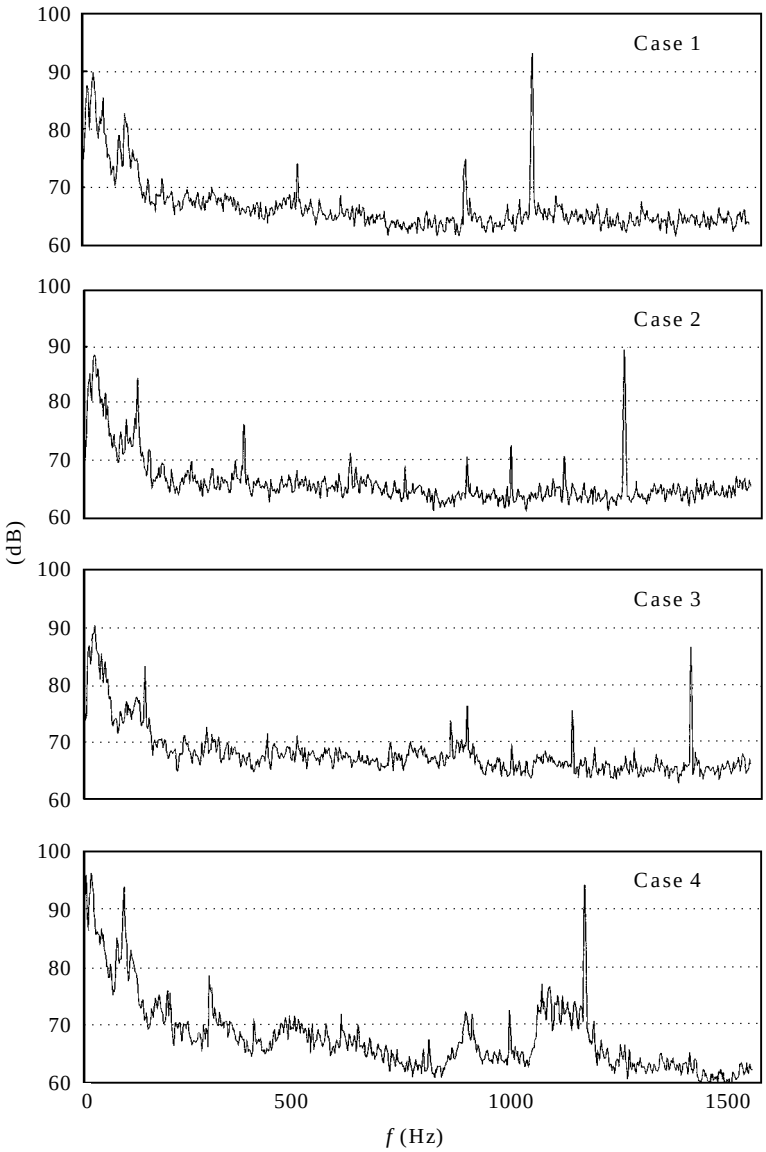

Figure 2. Acoustic frequency spectra for cases 1, 2, 3 and 4.

the fundamental mode increases rapidly approaching the trailing edge of the aerofoil. In this case there are no harmonics visible above the background level. (However in cases 1, 2 and 3 there are weak harmonics visible above the background level.) In Figure 4 the spectra display only broadband frequency over the entire aerofoil. Therefore, in case 5 there is no selective amplification of a single T–S wave with fixed frequency. In Figure 5 a fundamental mode is observed upstream of the trailing edge, but this mode is no longer visible at the trailing edge. The generation of tonal noise is dependent on an amplified T–S wave of discrete frequency propagating up to the trailing edge of the aerofoil. In case 6, LDA boundary-layer profiles show that transition from a laminar to a

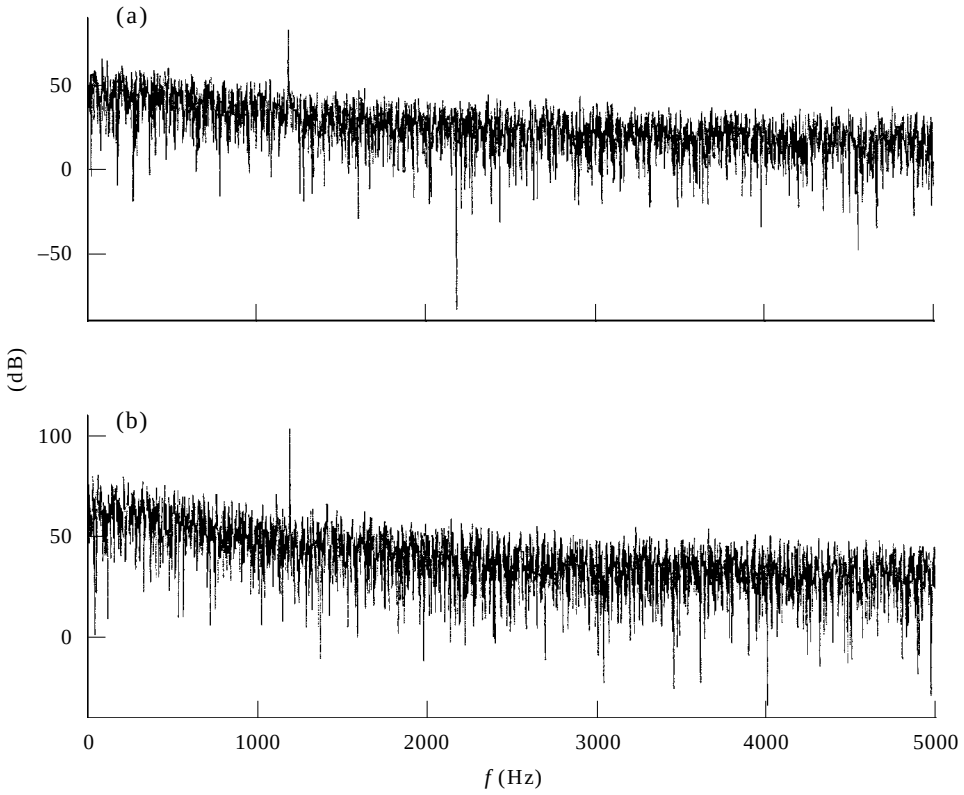

Figure 3. Frequency spectra taken at (a) 15 mm and (b) 0·5 mm upstream of the trailing edge of the aerofoil, for case 4.

turbulent flow occurs shortly upstream of the trailing edge, thus eliminating the T–S wave and the tonal noise.

In summary, the experimental results reveal the existence of an amplified boundary-layer instability wave (loosely referred to as a T–S wave) at the *same* frequency as the tone. The majority of the growth of the wave appears to occur close to the trailing edge of the aerofoil where the flow has separated and there exists a small region of reversed flow. The rapid growth of the discrete mode (over all other frequencies) is observed to start just before the flow separates. Previous papers have described a feedback loop between T–S and acoustic waves starting at a point where the flow first becomes unstable. In section 4 the flow is shown to become unstable at approximately 40% chord, but no discrete frequencies are detectable in the boundary layer until close to the trailing edge. The majority of the amplification of the T–S waves occurs close to the trailing edge of the aerofoil and this appears to be inconsistent with the aero-acoustic feedback model discussed in section 1.

All the frequency spectra shown have been taken inside the boundary layer. In addition, the frequency spectrum of the streamwise component of the flow was analyzed up to 100 mm above and below the aerofoil. Figure 6 (for case 1) is a contour plot of the amplitude of the discrete peak in the spectrum, at the

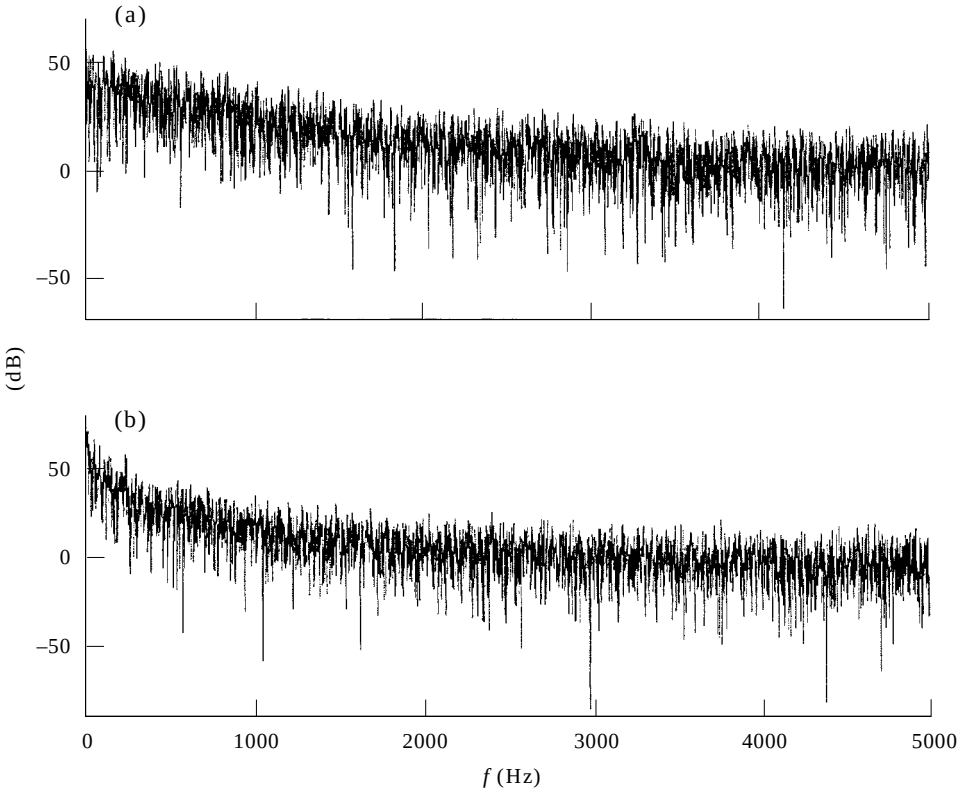

Figure 4. Frequency spectra taken at (a) 35 mm and (b) 0·5 mm upstream of the trailing edge of the aerofoil, for case 5.

frequency of the tone. (Note that the labels on each contour are the amplitude (in dB) *above* the background broadband level.)

Peak frequencies are detectable up to 150 mm upstream of the trailing edge (50% chord) on either side of the aerofoil. The approximately radial form of the contour lines (excluding the wake) is a characteristic of a field scattered by a sharp edge. On the suction surface (the top surface in Figure 6) the peak frequencies were undetectable within 5 mm of the surface because the boundary layer was turbulent. Hence, the wave-like pattern on the suction surface in Figure 6 has no physical significance, (and it is caused by the interpolation routine used to generate the contour lines).

In reference [13] flow visualization pictures of the wake of the aerofoil show the formation of a vortex street by the trailing edge, with vortices being shed alternately from the pressure and suction surfaces of the aerofoil. From Figure 6 and the flow visualization pictures one observes that the structure of the wake is remarkably organized, and the shedding frequency is controlled by the T–S waves on the pressure surface of the aerofoil. It is presumed that the quasi-periodic structure of the vortex street coupled with the boundary-layer structure on the pressure surface of the aerofoil accounts for the sharpness (narrow band) of the acoustic tone.

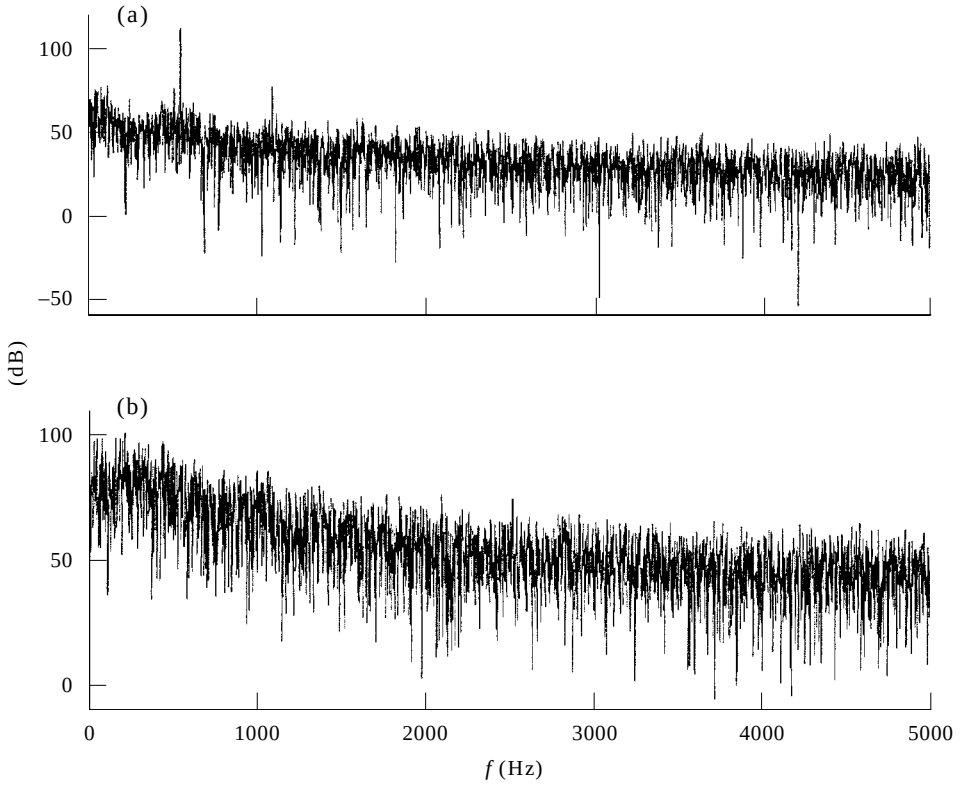

Figure 5. Frequency spectra taken at (a) 50 mm and (b) 0·5 mm upstream of the trailing edge of the aerofoil, for case 6.

Finally, note that the natural resonance frequencies of the aerofoil did not coincide with any of the observed tones. Nash (cf. reference [14], section 5.4) showed that tonal noise was not generated by structural vibrations of the aerofoil.

3. LINEAR STABILITY ANALYSIS

One of the aims of this study of tonal noise was to compare experimental and theoretical results. Assume in a first approximation that the boundary-layer disturbances remain approximately linear over the majority of the aerofoil chord. Then consider the stability of the flow by considering normal modes, assuming a disturbance may be expressed by a superposition of these modes.

From analyzing the experimental results, the boundary-layer disturbances appear suitable to be modelled by spatial modes of fixed frequency with *slowly* changing wavelengths to account for the development of the boundary layer. Following Bouthier [15] and Gaster and Grant [16], the development of a mode with fixed frequency in a laminar boundary layer was modelled simply by taking a stream function of the form

$$\psi(x, z) = \phi(z) \exp\{\mathrm{i}(\int \alpha(x)\, \mathrm{d}x - \omega t)\}, \tag{1}$$

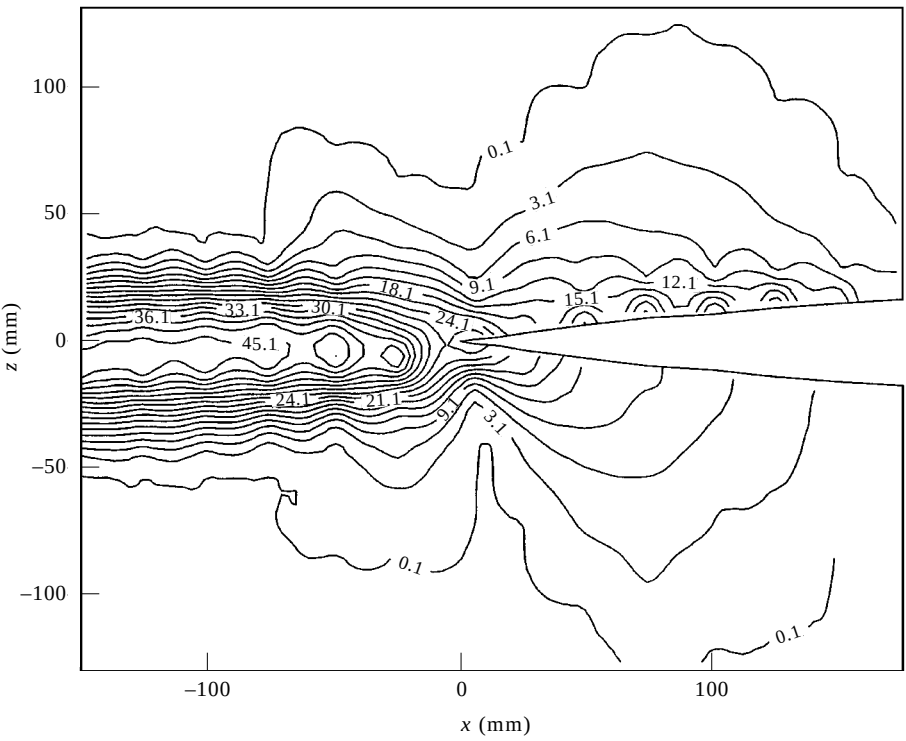

Figure 6. Contour plot of the amplitude of the streamwise peak frequency, for case 1. (Note in this figure the suction surface is the top surface.)

where $\alpha = \alpha_r + \mathrm{i}\alpha_i$ is the complex wavenumber, w the real frequency and (x, z) are Cartesian co-ordinates positioned such that the boundary is at $z = 0$. The amplification of a wave with fixed frequency and a *slowly* varying complex wavenumber α between $x = x_0$ and x_1 (where x_1 is downstream of x_0) will be

$$\frac{A(x_1)}{A(x_0)} = \exp\left\{-\int_{x_0}^{x_1} \alpha_i(x)\,\mathrm{d}x\right\}, \tag{2}$$

where $A(x)$ is the amplitude of the mode. By using equation (2), calculate the amplification of T–S waves in the pressure surface boundary layer of the aerofoil, over a range of frequencies, in order to compare the results of the linear stability analysis with the experimental data.

The wavenumber α is calculated by solving the Orr–Sommerfeld problem

$$\phi^{iv} - 2\alpha^2\phi'' + \alpha^4\phi = \mathrm{i}R\{(\alpha U - \omega)(\phi'' - \alpha^2\phi) - \alpha U''\phi\}, \tag{3}$$

$$\phi = \phi' = 0 \quad \text{at} \quad z = 0, \tag{4}$$

$$\left\{\begin{array}{l} \phi'' + (\alpha + \gamma)\phi' + \alpha\gamma\phi = 0 \\ \phi''' + (\alpha + \gamma\phi'' + \alpha\gamma\phi' = 0 \end{array}\right\} \quad \text{as} \quad z \to \infty, \tag{5}$$

where a prime denotes differentiation with respect to z, R is the Reynolds number and $\gamma = \sqrt{\alpha^2 + iR(\alpha - \omega)}$.

The Orr–Sommerfeld problem defined by equations (3)–(5) describes the development of infinitesimal disturbances in a boundary-layer flow with velocity profile $U(z)$. The Orr–Sommerfeld equation (3) may be solved for fixed (R, ω) to determine the wavenumber α of the least stable mode at any point in the (R, ω)-plane. The Orr–Sommerfeld equation is a stiff, differential eigenvalue problem which was solved by following the method of compound matrices described by Ng and Reid [17].

In each case (cf. Table 1) the wavenumber α was calculated at 12 stations, indicated on Figure 1 by circles (○), and an expression $\alpha_i(x)$ was derived by fitting a least-squares polynominal through the data points. The amplification between stations 1 and 12 on the aerofoil was then given by equation (2). Station 1 was taken close to the maximum thickness point of the aerofoil (approximately 30% chord), and station 12 as close as possible to the trailing edge of the aerofoil.

Falkner–Skan boundary-layer profiles appear suitable to model the flow over an aerofoil because, by varying the Falkner–Skan parameter β, profiles over a range of pressure gradients may be considered. The Falkner–Skan boundary-layer is derived by considering a similarity solution of the boundary-layer equations with a free-stream velocity $U_\infty \propto x^{\beta/2-\beta}$. The problem is reduced to

$$f''' + ff'' + \beta(1 - f'^2) = 0, \tag{6}$$

$$f(0) = f'(0) = 0, \quad f'(\infty) = 1, \tag{7}$$

where a prime denotes differentiation with respect to the similarity variable $\zeta = z/g(x)$, and the boundary-layer velocity profile is given by $U = U_\infty f'$. The function $g(x) \propto \sqrt{\nu x/U_\infty}$ is a stretching function to allow for the gradual thickening of the boundary layer with distance downstream (where ν is the kinematic viscosity).

On varying the parameter β the solution of equations (6) and (7) will give the boundary layer for the flow over a rigid plate inclined at an angle of $\pi\beta/2$. For $\beta > 0$ there will be a favourable pressure gradient and for $\beta < 0$ an adverse pressure gradient. For $\beta = -0{\cdot}1988$ the shear stress at the boundary surface is zero and the Falkner–Skan profile is on the verge of separation. For $-0{\cdot}1988 < \beta < 0$ the profiles of one family of solutions of the Falkner–Skan problem all exhibit a small region of reversed flow close to the boundary surface—there is boundary-layer separation.

The shape of the boundary-layer profile over the aerofoil slowly changes because of the aerofoil curvature. At each station the velocity profile U is approximated by a Falkner–Skan profile, by matching the shape factor H. Both the displacement thickness δ^* and momentum thickness θ may be measured experimentally by using the LDA. For the Falkner–Skan boundary layer,

$$\delta^*(x) = (\nu x/U_\infty)^{1/2}(2 - \beta)^{1/2} \int_0^\infty (1 - f')\, d\zeta, \tag{8}$$

$$\theta(x) = (\nu x/U_\infty)^{1/2}(2-\beta)^{1/2}\int_0^\infty f'(1-f')\,\mathrm{d}\zeta, \tag{9}$$

where x, the distance from the leading edge of the rigid plate in the Falkner–Skan formulation, has *no* relation to the location of the station on the aerofoil. The shape factor $H = \delta^*/\theta$ is independent of x, and for each Falkner–Skan boundary-layer profile there exists a *unique* shape factor which may be calculated. At each station δ^* and θ were measured by using the LDA to calculate the shape factor H, and then the flow at that station was modelled by a Falkner–Skan boundary layer with the same shape factor.

At each station the characteristic length scale is assumed to be δ^*. Therefore, the Reynolds number $R = U_\infty\delta^*/\nu$ and non-dimensional frequency $\omega = 2\pi f\delta^*/U_\infty$ are introduced, which are used when solving the Orr–Sommerfeld problem in this stability analysis.

An alternative method considered was to compare the pressure gradients at each station on the aerofoil. However, pressure measurements were not available from the wind-tunnel experiments in this study. A prediction code (kindly supplied by Dr J. Gaydon, Department of Aerospace Engineering, University of Bristol) was used to predict the pressure gradient. The code was only able to predict the pressure gradient where the flow was attached. The relative error between the predicted and the Falkner–Skan pressure gradient at each station was approximately 20–30%. Conclusions from the comparison between the predicted and theoretical pressure gradients are difficult because the pressure gradients could not be measured. Therefore the accuracy of the predicted pressure gradients is unknown. However, on matching the shape factor of the theory to the measured shape factor of the experiment, the pressure gradient predicted theoretically seems to be consistent with the experiment.

Several assumptions are made in this model. Firstly, in the Orr–Sommerfeld problem one assumes a parallel, bounded, basic flow $U(z)$. The theory is commonly utilized to investigate the development of quasi-parallel, semi-infinite flows such as a boundary layer. The quasi-parallel flow approximation assumes that over a finite length scale the basic flow is unchanged. Calculations for the cases in Table 1 indicate that the growth of the displacement thickness δ^* over one T–S wavelength λ_{TS} is less than 10% up to approximately 40 mm upstream of the trailing edge of the aerofoil. This is slightly upstream of the region of separated flow on the aerofoil. After flow separation the profiles "change" more rapidly and the validity of the calculations close to the trailing edge are questionable.

Secondly, the classical boundary-layer equations may break down at separation where the height of the region of reversed flow is comparable with the boundary-layer thickness. In this paper separation is defined as the onset of reversed flow. It is assumed that the onset of separation is close to the trailing edge of the aerofoil, and the height of the region of reversed flow remains small enough to disregard the effect of a possible singularity in the boundary-layer equations.

Finally, the flow is assumed to remain *stable* until at least station 1 on the aerofoil. Clearly the flow around the leading edge is not quasi-parallel. There will be a stagnation point at the "nose" of the aerofoil and instabilities may develop there. However, there exist strong favourable pressure gradients around the nose of the aerofoil which accelerate the flow and plausibly dampen any instabilities associated with the stagnation point. Therefore, the flow is assumed to be stable at the start of the region of quasi-parallel flow.

4. RESULTS

Results are presented for the six cases shown in Table 1. Figure 7 shows plots of the marginal stability curves ($\alpha_i = 0$) at stations 1 to 12 for case 4. The marginal curve for each station is labelled. The circles (○) denote the location in the (R, ω)-plane of a T–S wave, at the frequency of the tone, at the 12 stations along the aerofoil.

Figure 8 shows plots of the growth rate $-\alpha_i$ against frequency f at stations 1 to 12 for case 4. The growth rate curve for each station is labelled. The solid vertical line is the frequency of the tone. The two vertical dashed lines are the frequencies with maximum growth rate at stations 8 and 9—the relevance of these lines is discussed in section 4.1.

The marginal stability and growth rate curves for tonal cases 1, 2 and 3 are similar to Figures 7 and 8 (and hence are not presented in this paper).

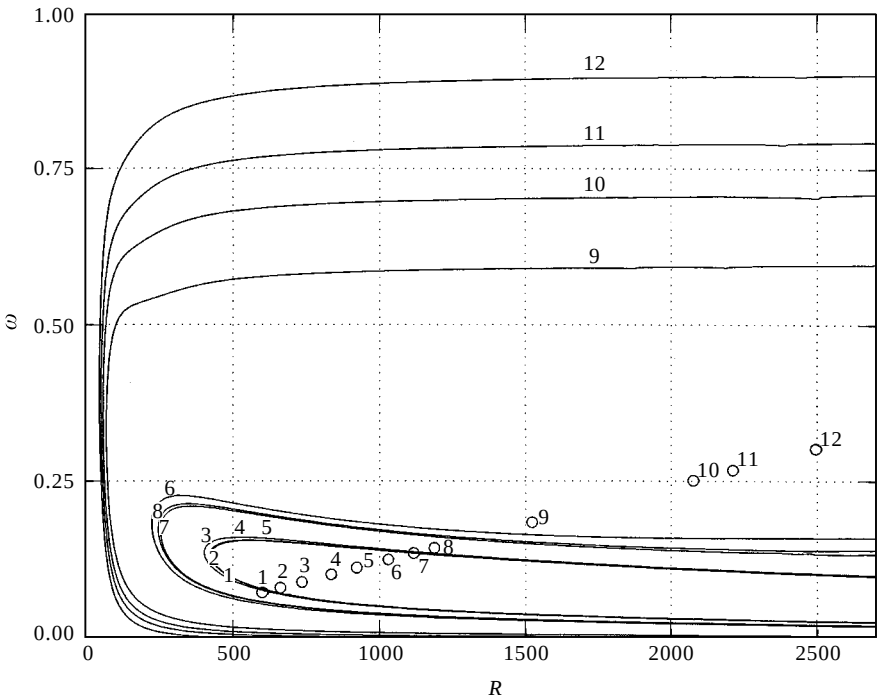

Figure 7. Marginal stability curves for case 4. The location in the (R, ω)-plane of a T–S wave with frequency 1192 Hz is denoted by ○ at stations 1 to 12.

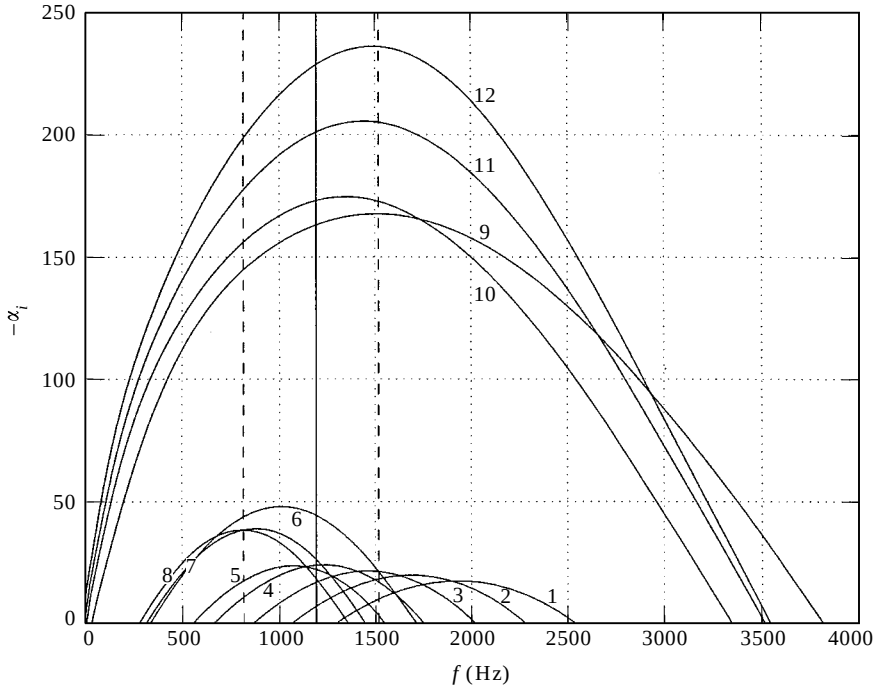

Figure 8. Growth rate curves for case 4.

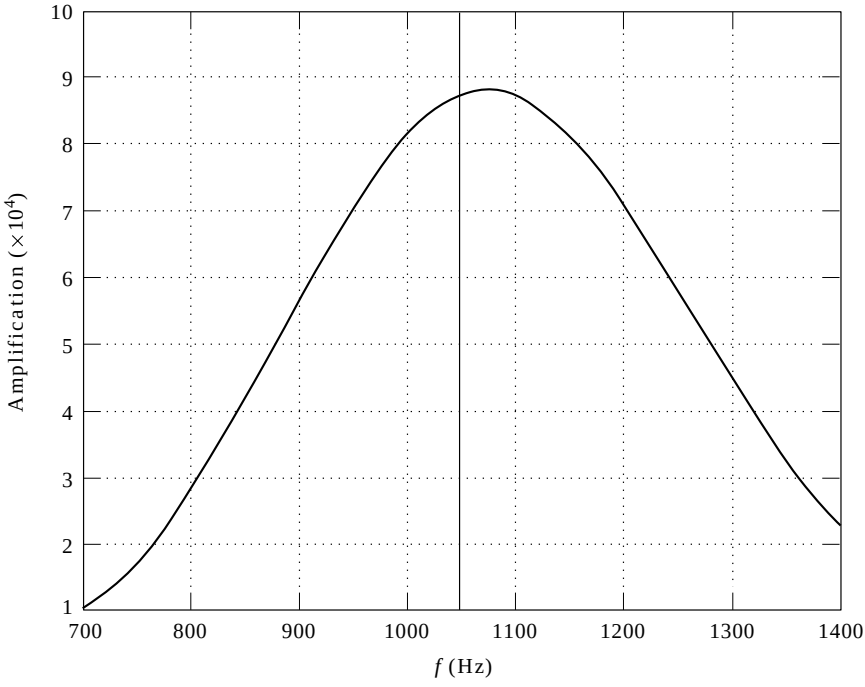

Figure 9. Amplification of T–S waves with fixed frequency 1048 Hz for case 1.

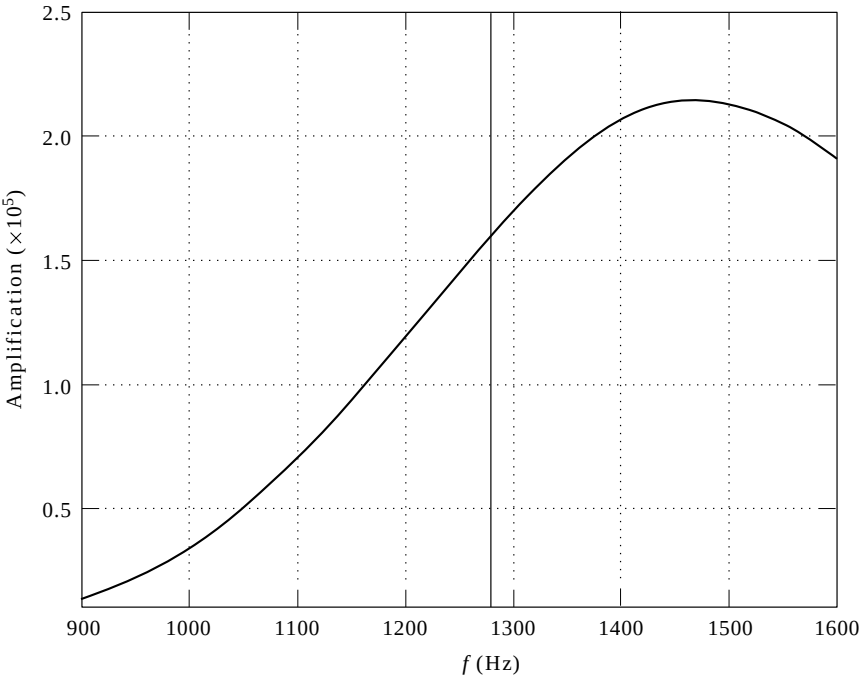

Figure 10. Amplification of T–S waves with fixed frequency 1280 Hz for case 2.

Figures 9–14 show plots of the amplification (2) of T–S waves with fixed frequency over the aerofoil for cases 1–6. Once again the solid vertical line is the frequency of the tone.

4.1. TONAL CASES: 1, 2, 3 AND 4

Figures 7 and 8 clearly show the change in the stability characteristics of the velocity profiles with streamwise location over the aerofoil. There are several points to note. In Figure 7, downstream of station 2 the frequency of the tone, 1192 Hz, translates to an *unstable* boundary-layer frequency. In this case, 1192 Hz is a *stable* frequency at station 1. The assumption that instabilities associated with the leading edge do not interfere with the development of instabilities between station 1 and the trailing edge appears reasonable.

The structure of the marginal curves changes between stations 8 and 9. From stations 1–8 there is a narrow band of unstable frequencies between the lower and upper branches of the marginal curves. The upper and lower branches appear to converge as $R \to \infty$. From stations 9–12 there is a broad band of unstable frequencies between the lower and upper branches of the marginal curves. Now the branches of the marginal curves do not appear to converge as $R \to \infty$. On several of the curves (notably at station 9) there is a "kink" located on the upper branch, close to the "nose" of the marginal curve. The relevance of these observations are discussed soon.

In Figure 8, the growth rates associated with stations 1–8 are considerably less than the corresponding growth rates at stations 9–12. From stations 1–8 the

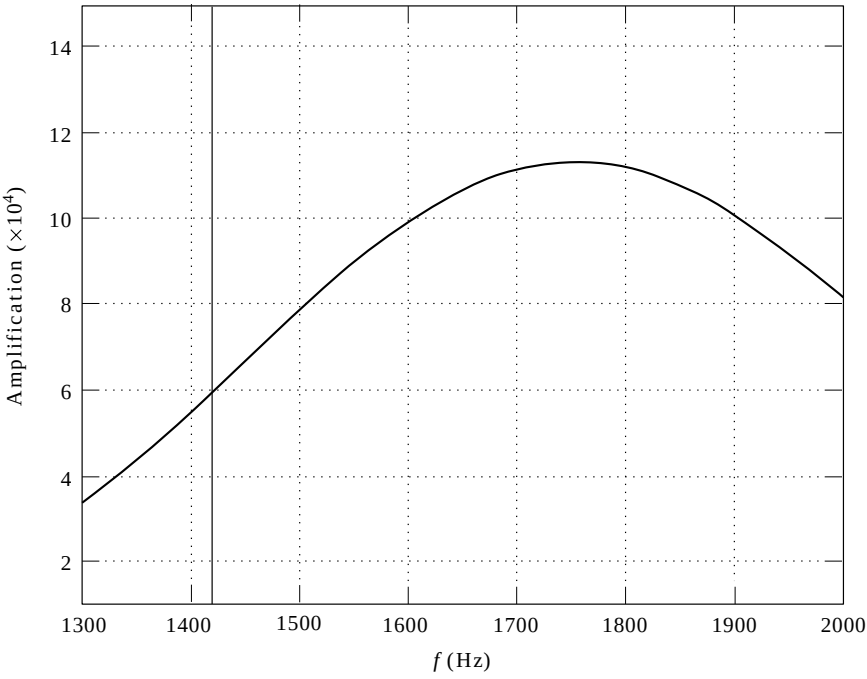

Figure 11. Amplification of T–S waves for case 3.

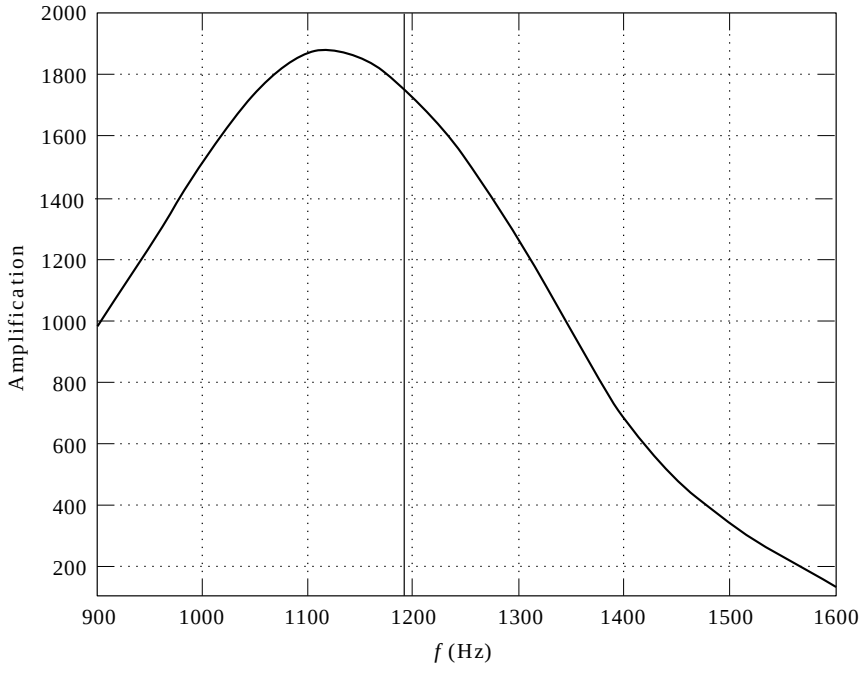

Figure 12. Amplification of T–S waves for case 4.

frequency of the mode with the maximum growth rate *decreases* at successive stations. The frequency of the mode with maximum growth rate at station 8 (denoted by a vertical dashed line) is *less* than 1192 Hz, the frequency of the tone. The frequency of the mode with the maximum growth rate at station 9 (also denoted by a vertical dashed line) is *greater* than 1192 Hz. Thus, the frequency of the tone is bound by the frequency of the modes with maximum growth rate at stations 8 and 9. Between stations 8 and 9 there is a dramatic change in the stability characteristics with large amplification of T–S waves predicted downstream of station 9.

Figure 12 shows remarkable agreement between the linear stability analysis and the experimental results. A mode with frequency about 1100 Hz is amplified over and above all other frequencies. The prediction error is less than 10%. Figures 9–11 show similar amplification curves for the tonal cases involving the NACA 0012 aerofoil. The prediction error is negligible in case 1, and approximately 13 and 23% in cases 2 and 3, respectively.

The prediction error in all the cases increases with the free-stream velocity U_∞. Typically the growth rates of the modes increase with R (and therefore with increasing U_∞). Thus, the inherent assumption that the disturbances remain linear between stations 1 and 12 is more questionable as the free-stream velocity increases.

The amplification factor in case 4 is only about 2000 compared with up to 200 000 on the NACA 0012 aerofoil. However, the growth rates appear to be of similar magnitude. The difference in the amplification appears to be due to the different shape and chord length of the aerofoils. The amplification (2) was

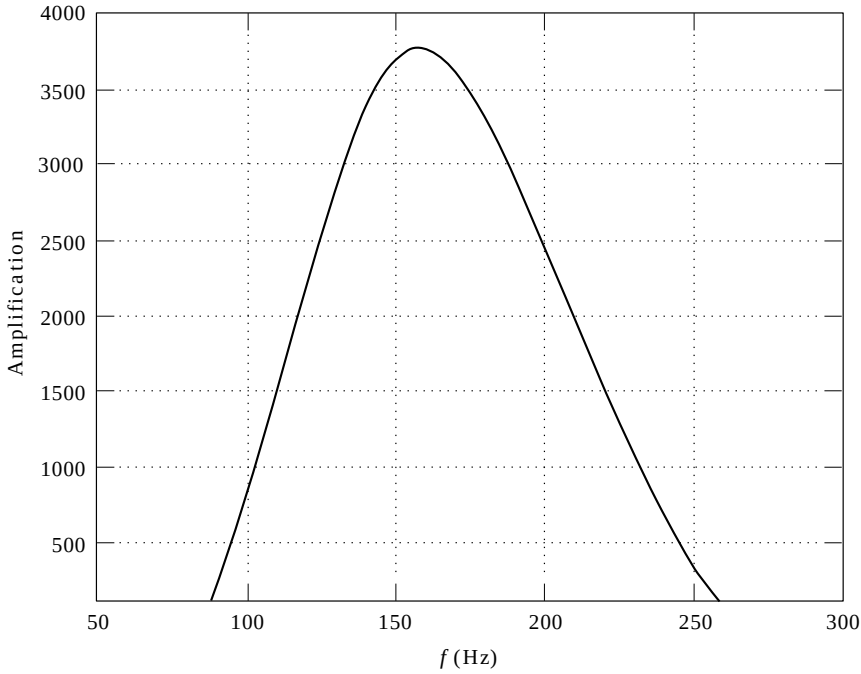

Figure 13. Amplification of T–S waves with fixed frequency (no tone) for case 5.

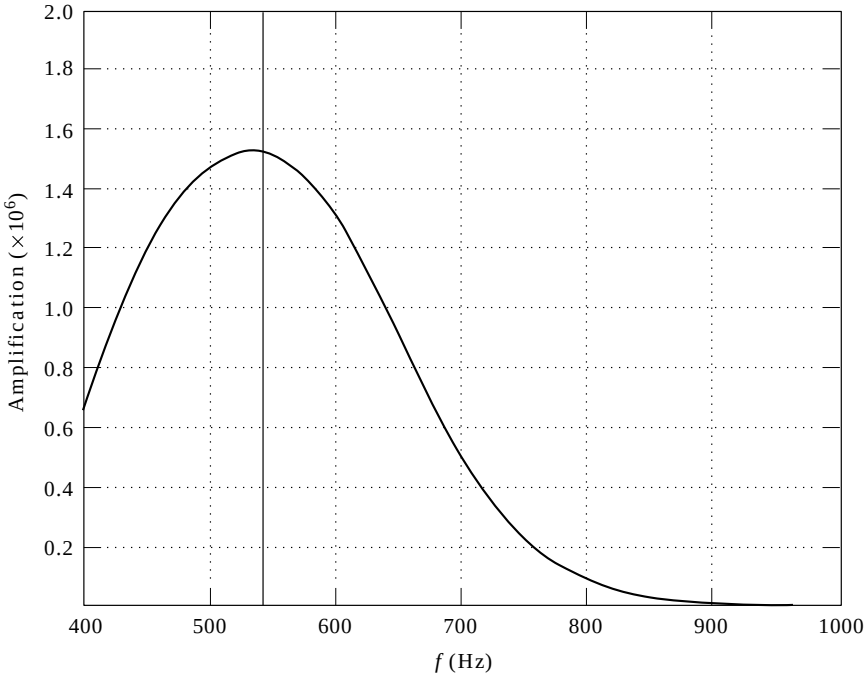

Figure 14. Amplification of T–S waves with fixed frequency (no tone) for case 6.

calculated by integrating the growth rate over 210 mm for the NACA 0012 aerofoil compared with 160 mm for the FX79 W151; thus, in general the amplification factors between different aerofoils are not comparable.

However, the description of the development of the flow remains the same for both aerofoils (and it is assumed that it is applicable to many aerofoil profiles where the flow remains quasi-parallel up to the trailing edge). It is proposed that the development of the boundary-layer disturbances is controlled by two different mechanisms of instability. The nature of the dominant mechanism of instability, governing the development of the flow, changes close to the point of flow separation. (In case 4 the change in the mechanism of instability is observed between stations 8 and 9.)

The viscous mechanism of instability proposed by Tollmien and Schlichting is well known. Viscous forces modify the phases of the velocity perturbations which lead to positive Reynolds stresses, enabling the transfer of energy from the mean-flow to the disturbance. The transfer of energy is determined by the product of the Reynolds stress and the mean-velocity gradient. These disturbances are known as Tollmien–Schlichting (T–S) waves. At large R there are two regions in the boundary layer where viscous effects are significant, namely the viscous wall layer and critical layer. The viscous wall layer is located by $z = 0$, whereas the critical layer is centred about $z = z_c$, where $U(z_c) = \Re\{w/\alpha\}$.

The stability characteristics of the flow of an inviscid fluid depend largely on the location of any inflexion points ($U'' = 0$). As $R \to \infty$ the stability of the flow is governed by inviscid dynamics described by the Rayleigh equation

$$(\alpha U - \omega)(\phi'' - \alpha^2 \phi) - \alpha U'' \phi = 0. \tag{10}$$

On using equation (10), Rayleigh's inflexion-point theorem states that a *necessary* condition for instability of an inviscid, bounded flow is the existence of an inflexion point, away from the boundary walls. Further, for unbounded shear flows an inflexion point in the profile is a *necessary* and *sufficient* condition for instability. Upon using this extension of Rayleigh's theorem, Falkner–Skan boundary-layer profiles with an inflexion point sufficiently away from the boundary will be unstable as $R \to \infty$ (this is observed in Figure 7 for the marginal curves downstream of station 9). The inflexion point must be located sufficiently away from the boundary so that the profile may locally be approximated by an unbounded shear layer.

Healey [18] investigated the dominant instability mechanism for boundary-layer flows under the influence of a small adverse pressure gradient (i.e., for Falkner–Skan profiles with β small and negative). He showed there exists a "kink" on the upper branch of the marginal stability curve for the Blasius boundary layer ($\beta = 0$) at $R \approx 10^5$. For large R on the lower branch, and up to the "kink" on the upper branch, the boundary layer had a triple-deck structure. After the "kink" on the upper branch the boundary layer had a quintuple-deck structure. In a triple-deck boundary layer the critical point z_c lies inside the viscous wall layer, but in a quintuple-deck the critical layer and viscous wall layer are separate. (Note that from the Rayleigh equation (10), the critical point z_c and the inflexion point will coincide where $R = \infty$.)

Healey plotted constant growth rate contours for Falkner–Skan profiles with a small adverse pressure gradient. After the "kink" in the marginal curve the contours below the upper branch were nearly horizontal, corresponding to inviscid waves because they were independent of R. For large R the inflexion point is located close to z_c, and therefore after the "kink" in the marginal curve the inflexion point will be outside the viscous wall layer, enabling instabilities to be dominated by inviscid dynamics. With stronger adverse pressure gradients the "kink" on the upper branch of the marginal curve moves to lower R. An increasingly large region between the upper and lower branches of the marginal curve will be dominated by inviscid instabilities. Also, the growth rates associated with the inviscid instabilities may typically be an order of magnitude larger than the corresponding growth rates for viscous instabilities.

Following the results by Healey, it is proposed that there is a change in the dominant mechanism of instability from viscous to inviscid dynamics. In Figures 7 and 8 this change is readily observed to occur between stations 8 and 9. Initially the perturbation energy is generated by the Reynolds stresses in the viscous wall layer. Further downstream, the inflexion point is located sufficiently outside the viscous wall layer such that the growth of the perturbation will now be governed by the inviscid dynamics of the inflexion-point profile. To remove the inflexion point sufficiently from the viscous wall layer, flow separation is

required. The inflexion point will lie *above* the region of reversed flow, and hence the large amplification which is required to initiate the tonal noise is dependent on the flow separating *near* the trailing edge of the aerofoil.

In Figure 8 the vertical dashed lines show the frequencies of the modes with maximum growth rate near the end of the viscous region and at the beginning of the inviscid region. We propose that the frequency of the mode with maximum amplification is *selected* between stations 8 and 9 (in this case). The majority of the amplification occurs in the inviscid region; however, if the frequency is selected near the *beginning* of this region then a linear analysis appears suitable to use as a first approximation when predicting the tonal frequency.

Tonal noise is dependent on the free-stream velocity U_∞ and the angle between the aerofoil and the oncoming stream. In these experiments, tonal noise was detected for $20\ \text{ms}^{-1} < U_\infty < 60\ \text{ms}^{-1}$, and when the aerofoil was placed at an angle between 2° and 5° to the oncoming stream (NACA 0012 aerofoil). Examples are now discussed where $U_\infty < 20\ \text{ms}^{-1}$ (case 5, section 4.2), $U_\infty > 60\ \text{ms}^{-1}$ (section 4.3) and the angle of attack is 0° (case 6, section 4.4), to enhance understanding of the tonal noise mechanism.

4.2. NO-TONE CASE 5

Figure 4 shows the frequency spectra taken in the centre of the boundary layer at (a) 35 mm and (b) 0·5 mm upstream of the trailing edge of the aerofoil, for case 5 where $U_\infty = 8\ \text{ms}^{-1}$. They both show frequency in a broad band with no discrete peaks anywhere in the boundary layer. In this case there is no selective large amplification of a mode of discrete frequency, and without this amplification, there is no tonal noise.

However, for case 5 the LDA boundary-layer profiles clearly show a large region of reversed flow near the trailing edge of the aerofoil. In section 4.1 it was proposed that the large amplification of the boundary-layer waves depends on the flow's separating near the trailing edge–this case appears to contradict this assumption.

From Figure 13 it may be predicted that a mode with frequency about 180 Hz should be detected in the boundary layer. However, on comparing with tonal cases 1, 2 and 3 the amplification is relatively weak, and is only over a narrow band of frequencies. It is assumed that the amplification is not sufficient to initiate the resonance mechanism generating tonal noise.

The weaker amplification is attributed to the reduction in the growth rates over the aerofoil. At the trailing edge the Reynolds number $R \approx 2500$ compared with $R \approx 3000$ in the tonal cases 1, 2 and 3. At lower R the growth rate $-\alpha_i$ is less, and thus the total amplification will dramatically decrease. With increasing R (and therefore free-stream velocity U_∞) the amplification will increase until reaching some critical level where the amplitude of the perturbations is sufficient to initiate tonal noise.

4.3. NO-TONE CASE FOR HIGH U_∞

For $U_\infty > 60\ \text{ms}^{-1}$ the LDA boundary-layer profiles clearly show that the flow on the pressure surface of the aerofoil is turbulent at the trailing edge. The tonal

noise mechanism is dependent on the existence of a large amplitude boundary-layer instability wave, at the same frequency, propagating up to the trailing edge of the aerofoil. A fully developed turbulent boundary layer would destroy any discrete frequency structure generated upstream of the transition point. For high free-stream velocities a linear stability analysis of the flow over the aerofoil is not possible because the assumption of linearity over the majority of the chord is no longer valid.

Transition from a laminar to turbulent flow is a gradual process as the free-stream velocity increases. The onset of turbulence has to be far enough upstream of the trailing edge to have a sufficient distance to destroy the boundary-layer waves. The experiments indicate that the region of reversed flow is compressed as the free-stream velocity increases. At high enough free-stream velocities the region of reversed flow will be very thin and the boundary layer will re-attach *before* the trailing edge. The flow propagating over the region of reversed flow will be very unstable and transition to a turbulent boundary layer will occur on or shortly after re-attachment.

At high free-stream velocities ($U_\infty \approx 60\ \mathrm{ms}^{-1}$) when tonal noise was still detected, the LDA boundary-layer profiles close to the trailing edge of the aerofoil do not show any reversed flow. However, large amplitude disturbances are still detected, at the frequency of the tone. From section 4.1 it is proposed that at high free-stream velocities flow separation is not necessary to enable disturbances to be controlled by the inflexion point in the boundary-layer profile. An improved description of the mechanism generating tonal noise would be that, the large amplification of boundary-layer waves is dependent on the disturbances being controlled by the inviscid dynamics of inflexional profiles upstream of the trailing edge of the aerofoil. However, over the majority of free-stream velocities when tonal noise is detected, flow separation (and therefore a small region of reversed flow) is necessary to enable the flow to be dominated by the inviscid dynamics of an inflexional profile.

It is proposed that tonal noise will not be detected when the transition to turbulence occurs sufficiently far upstream of the trailing edge of the aerofoil. The transition point depends upon the free-stream velocity and the angle between the aerofoil and the oncoming stream (see section 4.4).

4.4. NO-TONE CASE 6

When the NACA 0012 aerofoil was placed parallel to the oncoming stream there was no tonal noise detected *for all* free-stream velocities. For case 6 the LDA boundary-layer profiles show there is flow separation 60 mm upstream of the trailing edge of the aerofoil, and that transition from a laminar to turbulent boundary layer occurs far upstream of the trailing edge. (For case 6 the flow re-attaches 35 mm upstream of the trailing edge.)

Figure 5 shows that 50 mm upstream of the trailing edge a mode with frequency 542 Hz was detected in the boundary layer, approximately 30 dB above the background broadband level. By the trailing edge this was destroyed by the onset of turbulence and the frequency spectrum was entirely broadband.

In Figure 14, the amplification is calculated up to a station located 35 mm upstream of the trailing edge of the aerofoil, where the flow is still approximately laminar. In case 6, the large amplification of the boundary-layer instabilities occurs further upstream than in cases 1–4. In this case it is predicted that if the transition were prevented then a tone of 542 Hz would be detected. (The frequency prediction error is low because U_∞ was only 17 ms^{-1}.)

In this case the free-stream velocity is relatively low (i.e., compared with those discussed in section 4.3) and the mechanism controlling the onset of turbulence is different. For high free-stream velocities the onset of turbulence may be viewed as primarily a Reynolds number effect. In case 6 the free-stream velocity U_∞ (and hence R) is much lower and the onset of turbulence is now controlled by the pressure gradients close to the trailing edge of the aerofoil.

The pressure gradients around the aerofoil are related (locally) to the curvature of the profile. There are strong favourable pressure gradients around the blunt leading edge of the aerofoil where the curvature is high. The angle between the aerofoil and the oncoming stream alters the local curvature of the aerofoil surface with respect to the flow. The region of interest is approximately the final 25% of the chord, because tonal noise is dependent on the region of separated flow being located *close* to the trailing edge of the aerofoil.

When the angle between the aerofoil and the oncoming stream is greater than about 5° there will be no adverse pressure gradient on the pressure surface of the aerofoil. Therefore, amplification of the boundary-layer instability waves will be predominantly a viscous mechanism and the amplification will not be sufficient to initiate tonal noise. When the angle is very small (i.e., less than about 2°) the local curvature *close to the trailing edge* is greater than when the aerofoil is inclined at an angle between about 2° and 5° to the oncoming stream. With a very small angle the adverse pressure gradient close to the trailing edge is increased, and flow separation is located further upstream of the trailing edge than when the angle of the aerofoil to the oncoming stream is between about 2° and 5°.

Positioning the aerofoil at an angle between about 2° and 5° locates the flow separation close enough to the trailing edge to ensure that the flow remains approximately laminar up to the trailing edge. (We say "approximately laminar" because the flow may be transitional at, or slightly before, the trailing edge, but the turbulence is not fully developed, and this ensures that the frequency spectrum still contains the discrete peak.)

5. DISCUSSION

The aero-acoustic feedback models proposed by Tam [2], Wright [3], Longhouse [4], Fink [5] and Arbey and Bataille [6] may all be simplified by breaking down each model into the following three components: (1) formation of T–S waves in the pressure surface boundary layer; (2) generation of sound through the diffraction of the T–S waves at the trailing edge of the aerofoil; (3) feedback (i.e., transmission of the sound upstream and generation of more T–S

waves). Tonal noise will occur only when all three components are present. To suppress the tonal noise, at least one of the components must be removed from the system.

The generation of sound by diffraction at a sharp edge has been investigated by numerous authors (e.g., Ffowcs-Williams and Hall [19] investigated the sound field radiated by a distribution of turbulent eddies close to the edge of a half-plane). Aizin [20] investigated the generation of sound by a T–S wave passing over a sharp edge. He considered the diffraction of a T–S wave at the end of a flat plate in a uniform flow, by using the Wiener–Hopf technique. The problem for low Mach number flows was solved in two stages; firstly by solving the problem of a T–S wave incident on the edge in the near field, assuming incompressibility, and then by matching with the solution of the wave equation in the far field. Aizin derived an analytical expression for the acoustic potential in the far field (i.e., for radial distance $r \gg 1$ where the sharp edge is located at $r = 0$). The sound field had the *same* frequency as the T–S wave in the boundary layer and was directly proportional to the pressure exerted by the T–S wave at the sharp edge. The sound field contours had a characteristic cardioid shape with the cusp at $r = 0$.

An aerofoil is a slender body, and on assuming it is sufficiently long (i.e., chord length $\gg \lambda_{TS}$), the aerofoil may be replaced by a flat plate. Thus, in principle the analysis by Aizin may be used to solve part (2) in the aero-acoustic feedback model outlined previously. However, this analysis precludes parts (1) and (3) in the model.

The development of boundary-layer instability waves over the aerofoil has been discussed in section 4. The selection of a single mode, and its subsequent large amplification appears to be determined by the dynamics close to the point of flow separation. The frequency "selected" for amplification will remain the most amplified frequency up to the trailing edge of the aerofoil. In other words, from an initial set of unstable discrete frequencies, one frequency will eventually dominate. Linear theory predicts the frequency of the mode reasonably well because the frequency is "selected" in a region where the theory is valid. Where the frequency is "selected" the nature of the dominant mechanism of instability is changing.

The large amplification of the boundary-layer waves leads to the formation of a vortex street in the wake of the aerofoil. Normally the frequency of the disturbances in the wake is *not* related to the frequency of the boundary-layer disturbances because the wake and the boundary layer are effectively decoupled. The development of infinitesimal disturbances in the boundary layer is described by the viscous Orr–Sommerfeld problem (3) whereas for the wake the inviscid Rayleigh problem (10) is used. However, at each resonance frequency the wake instabilities are controlled by the pressure surface boundary layer. It is reasonable to assume that the frequencies in the suction surface boundary layer are in a broad band. The frequency of the vortex street is determined by the amplification of a "selected" boundary-layer instability wave. Tonal noise is heard when the whole system is "singing" at one frequency.

In principle this is in agreement with Paterson *et al.* [1], who attributed the tonal noise to vortex shedding. However, it is concluded that the tonal noise mechanism is *not* the same as the constant Strouhal number problem for bluff bodies used by Paterson *et al.* The Strouhal number was *not* a constant in our investigation. The frequency of the boundary-layer instability waves and the vortex wake appears to be determined by the stability characteristics of the boundary-layer profile at stations located over approximately two-thirds of the aerofoil, not just the profile at the trailing edge.

The transformation of free-stream oscillations into small-amplitude disturbances in the boundary layer, namely boundary-layer receptivity, is commonly separated into two categories: natural and forced receptivity [21]. Natural receptivity occurs where the wavelengths of the boundary layer and external disturbances are not comparable. The most common example of this is sound. A wavelength conversion process is required because the external disturbances will not contain much energy at the wavelengths of the boundary-layer instabilities. Forced receptivity occurs where the wavelengths of the boundary layer and external disturbances are comparable. There will then be a direct coupling, i.e., a direct transfer of energy. An example of this would be a localized unsteady pressure field outside of the boundary layer.

Forced receptivity occurs more easily than natural receptivity. Natural receptivity occurs predominantly in two regions: at the leading edge and where the boundary layer changes rapidly. Natural receptivity does not occur in a parallel flow region where the Orr–Sommerfeld problem is valid. Hence, natural receptivity is usually associated with non parallel mean-flows. Dovgal *et al.* [12] commented that velocity profiles within a separation bubble are more receptive than flows similar to the Blasius boundary layer.

For case 1, note that the acoustic wavelength $\lambda_{ac} \approx 320$ mm compared with $\lambda_{TS} \approx 11$ mm. The aero-acoustic feedback loop model proposed a coupling between sound waves propagating upstream from the trailing edge, and T–S waves propagating downstream in the boundary layer. It, was proposed that the coupling began where the flow became unstable, that is where $R \approx R_c$ (where R_c is the critical Reynolds number), which in case 4 is close to station 2 (see Figures 1 and 7). However, the amplification of the boundary-layer instability waves is predominantly in the region of separated flow. This region is small compared with the aerofoil chord. The "critical point" on the aerofoil would appear to be close to the point of flow separation, not where $R \approx R_c$, i.e., not where the flow initially becomes unstable.

It is proposed that boundary-layer receptivity will be weak where $R \approx R_c$. There are no discrete peaks in the frequency spectra in the boundary layer between R_c and the separation bubble. There may be several T–S waves with different frequencies propagating downstream, but their amplitudes will be relatively small. Any coupling between sound and T–S waves where $R \approx R_c$ would appear to have negligible effect on the subsequent large amplification close to the trailing edge of the aerofoil. The results in this paper suggest, in particular Figure 6, that forced boundary-layer receptivity in the region containing the separation bubble is a more suitable feedback model.

Paterson *et al.* [1] observed a "ladder-like" frequency response. This has been attributed to phase changes around the aero-acoustic feedback loop. A "ladder-like" frequency structure was not readily observable in our experimental results, but tonal noise was still detected. The tones may simply be explained in terms of the amplification of boundary-layer instabilities and we believe that a *feedback loop* is not a necessary condition for the generation of tonal noise (although as discussed above, it is proposed that there will be some feedback about the separation bubble). However, the coupling between the boundary-layer and the wake instabilities together with an upstream feedback mechanism about the separation bubble provides a mechanism which results in the narrow band spectral characteristics of the acoustic tone.

The tonal noise mechanism proposed herein combines well-known concepts of trailing edge noise (see many of the references in this paper). Each aerofoil had a sharp trailing edge, but the location of a separation bubble close to the trailing edge facilitated the generation of vortices shed into the wake forming a quasi-periodic vortex street, perhaps more closely resembling the wake of an aerofoil with a blunt trailing edge.

Further insight may be gained by investigating the regions of absolute and convective instability. Bers [22] proposed that these regions may be identified by examining the dispersion relation between the wavenumber and frequency. Reversed flow may be associated with absolute instability because there is a mechanism for upstream effects. Koch [23] considered the wake behind a cylinder and found there was a small region of absolute instability close to the body. He proposed a frequency prediction method to estimate the vortex-shedding frequency. A spatio-temporal stability analysis may provide further insight into the frequency selection criterion, and the location (relative to the trailing edge) of the dominant source of the tonal noise.

Finally, in the Orr–Sommerfeld theory one assumes that the local flow extends unchanged on an infinite domain, that is $-\infty < x < \infty$. For $R > R_c$ there is a continuous band of unstable frequencies which are amplified. However, the flow is bounded by the constraints of the wind-tunnel and the chord length of the aerofoil. An alternative approach to the problem would be to discard the above local approximation and apply bifurcation theory to the flow as a whole.

By Serrin's theorem, for a small enough R there will exist a unique, stable, steady flow around the aerofoil. With increasing R, the steady flow will remain stable until $R = R_c$. Then a Hopf bifurcation will occur and the flow will bifurcate from a steady, stable flow to a periodic, stable flow. This is known as a super-critical bifurcation. It is a description of the onset of instability with the feedback, yet a description which tells us nothing about the mechanisms of instability. With further increases of R there may be more bifurcations resulting in quasi-periodic flow and eventually chaos and turbulence.

The linear results suggest that the Orr–Sommerfeld theory may be used to obtain an approximation to f, the frequency observed in the flow after the Hopf bifurcation. It is proposed that the flow will bifurcate to a frequency *close* to the frequency of the mode with maximum linear amplification over the aerofoil.

6. CONCLUSIONS

From the results in this paper, tonal noise is largely dependent on the existence of a separation bubble close to the trailing edge of the aerofoil. The aero-acoustic feedback models proposed by several previous authors have been discussed, and it is proposed that feedback is more likely to occur about the separation bubble.

The distinctive "piercing whistle" or "singing" tones radiated by the aerofoil are due to a coupling between the boundary layer and wake instabilities, where there exists a single resonance frequency. The frequency of the vortex-street in the wake is determined by the development of boundary-layer instability waves on the pressure surface of the aerofoil. A frequency prediction may be obtained by calculating the growth of spatially growing modes in the boundary layer. This differs from the classical approach which presumes a wake controlled phenomenon, predicting the frequencies by using a Strouhal number mechanism based on the wake thickness (similar to predicting the frequencies in the wake of a bluff body).

A simple model has been used, and some assumptions made which may be plausibly no better than a rough first approximation, yet the results do seem to describe the observations surprisingly well.

ACKNOWLEDGMENTS

We are grateful to Professor Philip Drazin for his advice and suggestions about this work, and for his critical comments during the preparation of this paper. We also thank the referees for their comments. The work was supported by grants from the EPSRC.

REFERENCES

1. R. W. PATERSON, P. VOGT, M. FINK, and C. MUNCH 1973 *Journal of Aircraft* **10** 296–302, Vortex noise of isolated airfoils.
2. C. K. W. TAM 1974 *Journal of the Acoustical Society of America* **55**, 1173–1177. Discrete tones of isolated airfoils.
3. S. E. WRIGHT 1976 *Journal of Sound and Vibration* **45**, 165–223. The acoustic spectrum of axial flow machines.
4. R. E. LONGHOUSE 1977 *Journal of Sound and Vibration* **53**, 25–46. Vortex shedding noise of low tip speed, axial flow fans.
5. M. R. FINK 1978 *Paper H3, presented at the 95th meeting of the Acoustical Society of America*. Fine structure of airfoil tone frequency.
6. H. ARBEY and J. BATAILLE 1983 *Journal of Fluid Mechanics* **134**, 33–47. Noise generated by airfoil profiles placed in a uniform laminar flow.
7. W. K. BLAKE 1986 *Mechanics of Flow-induced Sound and Vibration, II: Complex Flow-Structure Interactions*. New York: Academic Press.
8. W. K. BLAKE and J. L. GERSHFELD 1989 *Lecture Notes in Engineering: Frontiers in Experimental Fluid Mechanics* (M. Gad-el-Hak, editor) 457–532. Berlin: Springer. The aeroacoustics of trailing edges.
9. A. S. HERSH and R. E. HAYDEN 1971 *NASA CR*-114370. Aerodynamic sound radiation from lifting surfaces with and without leading-edge serrations.

10. M. V. LOWSON, S. P. FIDDES and E. C. NASH 1994 *AIAA* 94-0358 32*nd Aerospace sciences meeting and exhibit*, *Reno*. Laminar boundary layer aeroacoustic instabilities.
11. E. C. NASH and M. V. LOWSON 1995 *CEAS-AIAA 95-124 First Joint Aero-acoustics Conference*, *Munich*. Noise due to boundary layer instabilities.
12. A. V. DOVGAL, V. V. KOZLOV and A. MICHALKE 1994 *Progress in Aerospace Science* **30**, 61–94. Laminar boundary layer separation: instability and associated phenomena.
13. E. C. NASH, M. V. LOWSON and A. MCALPINE 1999 *Journal of Fluid Mechanics* **382**, 27–61. Boundary layer instability noise on aerofoils.
14. E. C. NASH 1996 *PhD thesis*, *Department of Aerospace Engineering*, *University of Bristol*. Boundary layer instability noise on aerofoils.
15. M. BOUTHIER 1972 *Journal de Mécanique* **11**, 599–621. Stabilité linéaire des écoulements presque parallèles, (premiére partie).
16. M. GASTER and I. GRANT 1975 *Proceedings of the Royal Society of London A* **347**, 253–269. An experimental investigation of the formation and development of a wave packet in a laminar boundary layer.
17. B. S. NG and W. H. REID 1979 *Journal of Computational Physics* **30**, 125–136. An initial value method for eigenvalue problems using compound matrices.
18. J. J. HEALEY 1998 *European Journal of Mechanics*, *B/Fluids* **17**, 219–237. Characterizing boundary-layer instability at finite Reynolds numbers.
19. J. E. FFOWCS-WILLIAMS and L. H. HALL 1990 *Journal of Fluid Mechanics* **40**, 657–670. Aerodynamic sound generation by a turbulent flow in the vicinity of a scattering half plane.
20. L. B. AIZIN 1992 Translated from *Prikladnaya Mekhanika*; *Tekhnicheskaya Fizika* **3**, 50–57. Sound generation by a Tollmien–Schlichting wave at the end of a plate in a flow.
21. E. J. KERSCHEN 1989 *AIAA Paper No*. 89–1109. Boundary layer receptivity.
22. A. BERS 1975 *Physique des Plasma* (C. DeWitt and J. Peyraud, editors) 117–215. Linear waves and instabilities.
23. W. KOCH 1985 *Journal of Sound and Vibration* **99**, 53–83. Local instability characteristics and frequency determination of self-excited wake flows.